# An extended SEIARD model for COVID-19 vaccination in Mexico: analysis and forecast

Ángel G. C. Pérez[1,*] David A. Oluyori[2]

[1] Facultad de Matemáticas, Universidad Autónoma de Yucatán, Mérida, Yucatán, Mexico
[2] Department of Mathematics, School of Physical Science, Ahmadu Bello University, Zaria, Kaduna State, Nigeria

**Abstract**

In this study, we propose and analyze an extended SEIARD model with vaccination. We compute the control reproduction number $\mathcal{R}_c$ of our model and study the stability of equilibria. We show that the set of disease-free equilibria is locally asymptotically stable when $\mathcal{R}_c < 1$ and unstable when $\mathcal{R}_c > 1$, and we provide a sufficient condition for its global stability. Furthermore, we perform numerical simulations using the reported data of COVID-19 infections and vaccination in Mexico to study the impact of different vaccination, transmission and efficacy rates on the dynamics of the disease.

## 1 Introduction

The COVID-19 pandemic, caused by the Severe Acute Respiratory Syndrome Coronavirus 2 (SARS-CoV-2) has caused a worldwide crisis due to its effects on society and global economy. Due to the absence of specific anti-COVID-19 medical treatments, most countries had been relying on non-pharmaceutical interventions, such as wearing of face masks, social/physical distancing, partial/total lockdown, travel restrictions, and closure of schools and work centres, in order to curtail the spread of the disease before December 2020. However, these measures have been insufficient to mitigate the pandemic globally as medical facilities were overstretched and death toll heightened.

Vaccination has been an effective strategy in combating the spread of infectious diseases, e.g., pertussis, measles, and influenza. Historically, the eradication of smallpox has been considered as the most remarkable success of vaccination ever recorded [1]. According to [2], vaccination is the process of administering weakened or dead pathogens to a healthy person or animal with the intent of conferring immunity against a targeted form of a related disease agent; the individuals having the vaccine-induced immunity can be

*Corresponding author.
E-mail addresses: agcp26@hotmail.com (A. G. C. Pérez), oluyoridavid@gmail.com (D. A. Oluyori)

distinguished from the recovered individuals by natural immunity. So far, the development and testing of vaccines against SARS-CoV-2 has occurred at an unprecedented speed and, in the last months, several vaccines have been approved for use in many countries, and their deployment is already underway. In a pandemic situation such as this, current preventive vaccines consisting of inactivated viruses do not protect all vaccine recipients equally as the protection conferred by the vaccine is dependent on the immune status of the recipient [3].

Over the past few decades, a large number of simple compartmental mathematical models with vaccinated population have been proposed in the literature to assess the effectiveness of vaccines in combatting the infectious diseases [2, 4–12]. With the recent development of anti-COVID vaccines, several models have been proposed to provide insight into the effect that inoculation of a certain portion of the population will have on the dynamics of the COVID-19 pandemic. For instance, an age- and region-structured model was proposed in [13] to simulate the rollout of a two-dose vaccination programme in the UK using the Pfizer–BioNTech and Oxford–AstraZeneca vaccines. Another model was studied in [14] to compare the outcomes of single-dose and two-dose anti-COVID vaccination regimes, however, this model does not distinguish between symptomatic and asymptomatic infections. Other COVID-19 models with vaccination have been proposed in [15–19].

The motivation of this study is derived from the work of the authors in [20, 21], who considered an SEIARD mathematical model to investigate the outbreak of the coronavirus disease (COVID-19) in Mexico. Therefore, in the present study, we incorporate the vaccination component to the model in [21] to derive an extended SEIARD model to examine the effectiveness of the COVID-19 jabs which are currently being deployed to many countries to help combat the raging pandemic situation.

The rest of this paper is organized as follows. In Section 2, we present the equations and assumptions of the extended SEIARD model with vaccination. In Section 3, we perform a theoretical analysis of the model, compute its control reproduction number and study the stability of the disease-free equilibria. In Section 4, we carry out numerical simulations using reported data on COVID-19 infections and vaccination in Mexico. Lastly, we provide some discussions and concluding remarks in Section 5.

# 2 Model formulation

To derive the mathematical model, we subdivide the unvaccinated population into susceptible ($S$), exposed ($E$), symptomatic infectious ($I$), asymptomatic infectious ($A$), and recovered ($R$). The number of individuals in each subpopulation at time $t$ is denoted by $S(t)$, $E(t)$, etc. Susceptible individuals become exposed by contact with symptomatic infectious individuals at a rate $\beta_1$ and by contact with asymptomatic infectious individuals at a rate $\beta_2$. The exposed individuals become infectious at a rate $w$: a proportion $p_1$ of them will show symptoms of the disease, while the rest remains asymptomatic. We assume that the symptomatic class has a disease-induced death rate, denoted by $\delta_1$ (our model does not consider deaths not related to COVID-19). Both symptomatic and asymptomatic infectious people recover at a rate $\gamma$.

We also assume that the susceptible population $S$ is vaccinated at a rate $v \geq 0$ (the

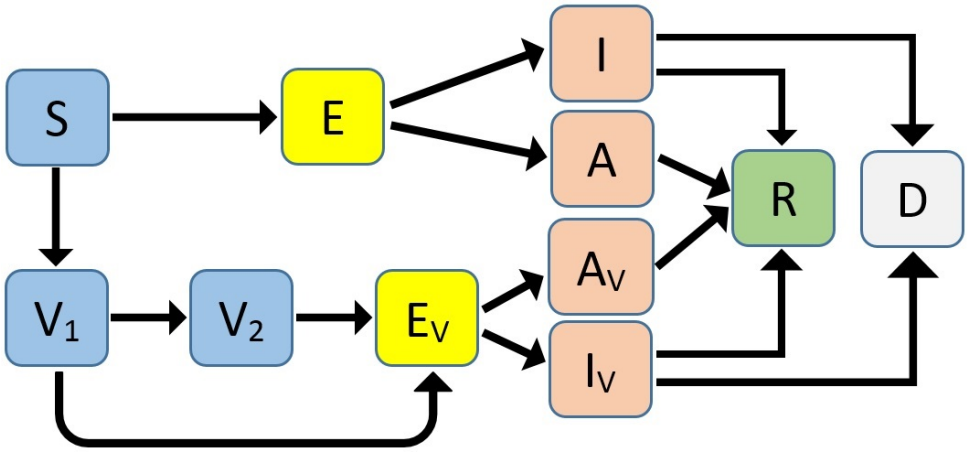


Figure 1: Flow diagram of the model with vaccination.

number of first doses administered per day at time $t$ is given by $vS(t)$). Individuals who have received only the first dose of the vaccine are included in the class $V_1$, and they move to the class $V_2$ upon receiving the second dose, which occurs at a rate $\theta$. Both $V_1$ and $V_2$ are considered susceptible. Since the vaccine does not completely remove the risk of infection, we also assume that the vaccinated population can become exposed ($E_V$), symptomatic infectious ($I_V$) and asymptomatic infectious ($A_V$). Individuals in the class $V_1$ (respectively, $V_2$) move to the class $E_V$ due to contact with symptomatic infectious persons at a rate $(1-\eta_1)\beta_1$ (respectively, $(1-\eta_2)\beta_1$) and by contact with the asymptomatic infectious at a rate $(1-\eta_1)\beta_2$ (respectively, $(1-\eta_2)\beta_2$), where $\eta_1$ is the efficacy of the vaccine after one dose ($\eta_2$ is the efficacy of the vaccine after two doses).

The population in the class $E_V$ becomes infectious at a rate $w$; we assume that the proportion of people from this class who become symptomatic infectious is $p_2$, which may be different from that of unvaccinated people due to the effect of the vaccine in reducing the severity of the infection. Likewise, the disease-induced death rate $\delta_2$ is lower for the vaccinated population. Individuals in the $I_V$ and $A_V$ classes also move to the $R$ class upon recovery from the disease at a rate $\gamma$.

We will denote by $N(t)$ the total population at time $t$, which is given by

$$N(t) = S(t) + E(t) + I(t) + A(t) + V_1(t) + V_2(t) + E_V(t) + I_V(t) + A_V(t) + R(t).$$

Hence, our model is described by the following system of differential equations:

$$
\begin{aligned}
\dot{S} &= -\frac{S}{N}\beta_1(I+I_V) - \frac{S}{N}\beta_2(A+A_V) - vS,\\
\dot{E} &= \frac{S}{N}\beta_1(I+I_V) + \frac{S}{N}\beta_2(A+A_V) - wE,\\
\dot{I} &= p_1 wE - (\delta_1+\gamma)I,\\
\dot{A} &= (1-p_1)wE - \gamma A,\\
\dot{V}_1 &= vS - (1-\eta_1)\frac{V_1}{N}\beta_1(I+I_V) - (1-\eta_1)\frac{V_1}{N}\beta_2(A+A_V) - \theta V_1,\\
\dot{V}_2 &= \theta V_1 - (1-\eta_2)\frac{V_2}{N}\beta_1(I+I_V) - (1-\eta_2)\frac{V_2}{N}\beta_2(A+A_V),\\
\dot{E}_V &= (1-\eta_1)\frac{V_1}{N}\beta_1(I+I_V) + (1-\eta_1)\frac{V_1}{N}\beta_2(A+A_V)\\
&\quad + (1-\eta_2)\frac{V_2}{N}\beta_1(I+I_V) + (1-\eta_2)\frac{V_2}{N}\beta_2(A+A_V) - wE_V,\\
\dot{I}_V &= p_2 wE_V - (\delta_2+\gamma)I_V\\
\dot{A}_V &= (1-p_2)wE_V - \gamma A_V,\\
\dot{R} &= \gamma(I+A+I_V+A_V).
\end{aligned}
\tag{1}
$$

We define an additional variable $D(t)$ that denotes the number of people deceased due to COVID-19, which is governed by the equation

$$\dot{D} = \delta_1 I + \delta_2 I_V. \tag{2}$$

The flow diagram of the model can be seen in Figure 1. The list of parameters and their interpretation is as follows:

- $\beta_1 > 0$: transmission rate by contact with symptomatic infectious individuals.
- $\beta_2 > 0$: transmission rate by contact with asymptomatic infectious individuals.
- $v \geq 0$: vaccination rate.
- $1/\theta$: time between the application of the first and the second dose of the vaccine.
- $\eta_1 \in [0,1]$: efficacy rate of the vaccine after the first dose.
- $\eta_2 \in [0,1]$: efficacy rate of the vaccine after the second dose.
- $1/w$: length of the latent period.
- $p_1 \in [0,1]$: proportion of infectious unvaccinated individuals that show symptoms of the disease.
- $p_2 \in [0,1]$: proportion of infectious vaccinated individuals that show symptoms of the disease.
- $\delta_1 \geq 0$: death rate of infectious unvaccinated individuals with symptoms.
- $\delta_2 \geq 0$: death rate of infectious vaccinated individuals with symptoms.
- $\gamma > 0$: recovery rate.

# 3 Theoretical analysis

In this section, we will derive some theoretical results for model (1). Since we are mainly interested in the long term behaviour of the epidemic, we will focus on the case when the vaccination campaign is over and hence the vaccination rate $v$ is zero, but the vaccinated subpopulations ($V_1$, $V_2$, $E_V$, $I_V$, $A_V$) may have positive initial values.

First, we will determine the disease-free equilibria of the model. It is easy to notice that system (1) does not have any equilibria when $v$ is positive. On the other hand, when $v$ is zero, model (1) has a continuum of disease-free equilibria (DFE), given by

$$P_0 : (S, E, I, A, V_1, V_2, E_V, I_V, A_V, R) \equiv (S^*, 0, 0, 0, 0, V_2^*, 0, 0, 0, R^*)\,,$$

where $S^* \geq 0$, $V_2^* > 0$ and $R^* > 0$. These equilibria represent the scenario when the anti-COVID vaccination program has ended, and a certain number of individuals $V_2^*$ has been vaccinated to achieve herd immunity in the population. We will compute the *control reproduction number* $\mathcal{R}_c$ of the model based on this expression for the DFE.

Using the notation in [22], we determine the matrix of new infections $\mathcal{F}$ and the transition matrix $\mathcal{V}$, considering only the infected compartments ($E$, $I$, $A$, $E_V$, $I_V$ and $A_V$). We have

$$\mathcal{F} = \begin{bmatrix} \frac{S}{N}\beta_1(I + I_V) + \frac{S}{N}\beta_2(A + A_V) \\ 0 \\ 0 \\ (1-\eta_1)\frac{V_1}{N}\left[\beta_1(I + I_V) + \beta_2(A + A_V)\right] + (1-\eta_2)\frac{V_2}{N}\left[\beta_1(I + I_V) + \beta_2(A + A_V)\right] \\ 0 \\ 0 \end{bmatrix}$$

and

$$\mathcal{V} = \begin{bmatrix} wE \\ -p_1 wE + (\delta_1 + \gamma)I \\ -(1-p_1)wE + \gamma A \\ wE_V \\ -p_2 wE_V + (\delta_2 + \gamma)I_V \\ -(1-p_2)wE_V + \gamma A_V \end{bmatrix}.$$

The derivative of $\mathcal{F}$ at a disease-free equilibrium $P_0$ is

$$F = \begin{bmatrix} 0 & \frac{S^*}{N^*}\beta_1 & \frac{S^*}{N^*}\beta_2 & 0 & \frac{S^*}{N^*}\beta_1 & \frac{S^*}{N^*}\beta_2 \\ 0 & 0 & 0 & 0 & 0 & 0 \\ 0 & 0 & 0 & 0 & 0 & 0 \\ 0 & (1-\eta_2)\frac{V_2^*}{N^*}\beta_1 & (1-\eta_2)\frac{V_2^*}{N^*}\beta_2 & 0 & (1-\eta_2)\frac{V_2^*}{N^*}\beta_1 & (1-\eta_2)\frac{V_2^*}{N^*}\beta_2 \\ 0 & 0 & 0 & 0 & 0 & 0 \\ 0 & 0 & 0 & 0 & 0 & 0 \end{bmatrix}$$

where $N^* = S^* + V_2^* + R^*$ denotes the total population at the equilibrium. The derivative

of $\mathcal{V}$ evaluated at $P_0$ is

$$V = \begin{bmatrix} w & 0 & 0 & 0 & 0 & 0 \\ -p_1 w & \delta_1+\gamma & 0 & 0 & 0 & 0 \\ -(1-p_1)w & 0 & \gamma & 0 & 0 & 0 \\ 0 & 0 & 0 & w & 0 & 0 \\ 0 & 0 & 0 & -p_2 w & \delta_2+\gamma & 0 \\ 0 & 0 & 0 & -(1-p_2)w & 0 & \gamma \end{bmatrix}.$$

It follows that

$$FV^{-1} = \begin{bmatrix} A_{11} & \frac{S^*\beta_1}{N^*(\delta_1+\gamma)} & \frac{S^*\beta_2}{N^*\gamma} & A_{14} & \frac{S^*\beta_1}{N^*(\delta_2+\gamma)} & \frac{S^*\beta_2}{N^*\gamma} \\ 0 & 0 & 0 & 0 & 0 & 0 \\ 0 & 0 & 0 & 0 & 0 & 0 \\ A_{41} & \frac{(1-\eta_2)V_2^*\beta_1}{N^*(\delta_1+\gamma)} & \frac{(1-\eta_2)V_2^*\beta_2}{N^*\gamma} & A_{44} & \frac{(1-\eta_2)V_2^*\beta_1}{N^*(\delta_2+\gamma)} & \frac{(1-\eta_2)V_2^*\beta_2}{N^*\gamma} \\ 0 & 0 & 0 & 0 & 0 & 0 \\ 0 & 0 & 0 & 0 & 0 & 0 \end{bmatrix},$$

where

$$\begin{aligned} A_{11} &= \frac{S^*}{N^*}\left[\frac{\beta_1 p_1}{\delta_1+\gamma} + \frac{\beta_2(1-p_1)}{\gamma}\right], \\ A_{14} &= \frac{S^*}{N^*}\left[\frac{\beta_1 p_2}{\delta_2+\gamma} + \frac{\beta_2(1-p_2)}{\gamma}\right], \\ A_{41} &= \frac{(1-\eta_2)V_2^*}{N^*}\left[\frac{\beta_1 p_1}{\delta_1+\gamma} + \frac{\beta_2(1-p_1)}{\gamma}\right], \\ A_{44} &= \frac{(1-\eta_2)V_2^*}{N^*}\left[\frac{\beta_1 p_2}{\delta_2+\gamma} + \frac{\beta_2(1-p_2)}{\gamma}\right]. \end{aligned}$$

The control reproduction number $\mathcal{R}_c$ of model (1) is given by $\mathcal{R}_c = \rho\left(FV^{-1}\right)$, where $\rho$ denotes the spectral radius. Hence,

$$\mathcal{R}_c = \frac{S^*}{N^*}\left[\frac{\beta_1 p_1}{\delta_1+\gamma} + \frac{\beta_2(1-p_1)}{\gamma}\right] + \frac{(1-\eta_2)V_2^*}{N^*}\left[\frac{\beta_1 p_2}{\delta_2+\gamma} + \frac{\beta_2(1-p_2)}{\gamma}\right]. \tag{3}$$

The quantity $\mathcal{R}_c$ measures the average number of new COVID-19 cases generated by a typical infectious individual introduced into a population where a fraction $V_2^*/N^*$ has been fully vaccinated using a vaccine with efficacy $\eta_2$.

According to [22, Theorem 2], we can obtain the following result about the control reproduction number.

**Theorem 1.** *The continuum of disease-free equilibria $P_0$ of system (1) with $v = 0$ is locally asymptotically stable if $\mathcal{R}_c < 1$, and it is unstable if $\mathcal{R}_c > 1$.*

The following theorem gives a sufficient condition for the global stability of the disease-free equilibria.

**Theorem 2.** *Suppose that*

$$\frac{\beta_1 p_1}{\delta_1+\gamma}+\frac{\beta_2(1-p_1)}{\gamma}<1 \quad \textit{and} \quad (1-\eta_2)\left[\frac{\beta_1 p_2}{\delta_2+\gamma}+\frac{\beta_2(1-p_2)}{\gamma}\right]<1. \tag{4}$$

*Then, the continuum of disease-free equilibria $P_0$ of system (1) with $v=0$ is globally asymptotically stable.*

*Proof.* Consider the following Lyapunov function:

$$\mathcal{L}=g_1E+g_2I+g_3A+g_4E_V+g_5I_V+g_6A_V+g_7V_1,$$

where

$$g_1=\gamma(\delta_1+\gamma), \quad g_2=\gamma\beta_1, \quad g_3=(\delta_1+\gamma)\beta_2, \quad g_4=\frac{\gamma(\delta_1+\gamma)}{1-\eta_2},$$
$$g_5=\frac{\gamma\beta_1(\delta_1+\gamma)}{\delta_2+\gamma}, \quad g_6=\beta_2(\delta_1+\gamma), \quad g_7=\frac{\gamma(\delta_1+\gamma)}{1-\eta_2}.$$

The time derivative of $\mathcal{L}$ evaluated at the solutions of system (1) with $v=0$ is given by

$$\begin{aligned}\dot{\mathcal{L}}=&\, g_1\left[\frac{S}{N}\beta_1(I+I_V)+\frac{S}{N}\beta_2(A+A_V)-wE\right]+g_2\big[p_1wE-(\delta_1+\gamma)I\big]\\
&+g_3\big[(1-p_1)wE-\gamma A\big]+g_4\Big[(1-\eta_1)\frac{V_1}{N}\beta_1(I+I_V)+(1-\eta_1)\frac{V_1}{N}\beta_2(A+A_V)\\
&+(1-\eta_2)\frac{V_2}{N}\beta_1(I+I_V)+(1-\eta_2)\frac{V_2}{N}\beta_2(A+A_V)-wE_V\Big]\\
&+g_5\big[p_2wE_V-(\delta_2+\gamma)I_V\big]+g_6\big[(1-p_2)wE_V-\gamma A_V\big]\\
&+g_7\left[-(1-\eta_1)\frac{V_1}{N}\beta_1(I+I_V)-(1-\eta_1)\frac{V_1}{N}\beta_2(A+A_V)-\theta V_1\right].\end{aligned}$$

After cancelling terms and simplifying, we obtain

$$\begin{aligned}\mathcal{L}=&\,\gamma\beta_1(\delta_1+\gamma)(I+I_V)\left(\frac{S}{N}+\frac{V_2}{N}-1\right)+\gamma\beta_2(\delta_1+\gamma)(A+A_V)\left(\frac{S}{N}+\frac{V_2}{N}-1\right)\\
&+w\gamma(\delta_1+\gamma)\left[\frac{\beta_1p_1}{\delta_1+\gamma}+\frac{\beta_2(1-p_1)}{\gamma}-1\right]E\\
&+\frac{w\gamma(\delta_1+\gamma)}{1-\eta_2}\left[\frac{\beta_1p_2(1-\eta_2)}{\delta_2+\gamma}+\frac{\beta_2(1-p_2)(1-\eta_2)}{\gamma}-1\right]E_V-\frac{\gamma\theta(\delta_1+\gamma)}{1-\eta_2}V_1.\end{aligned}$$

Since $S(t)+V_2(t)\le N(t)$ for all $t$, we have $\frac{S}{N}+\frac{V_2}{N}\le 1$. Combining this with the hypothesis (4), we can see that $\dot{\mathcal{L}}\le 0$, and $\dot{\mathcal{L}}=0$ if and only if $E(t)=0$ and $E_2(t)=0$. Substituting $E(t)=0$ and $E_2(t)=0$ in system (1) with $v=0$ shows that $(S,E,I,A,V_1,V_2,E_V,I_V,A_V,R)\to(S^*,0,0,0,0,V_2^*,0,0,0,R^*)$ as $t\to\infty$. Hence, the largest positively invariant set where $\dot{\mathcal{L}}=0$ is the continuum of disease-free equilibria. Therefore, by LaSalle's invariance principle, we conclude that $P_0$ is globally asymptotically stable. □

Table 1: Baseline values for the parameters used in the simulations.

| Parameter | Value | Source |
|---|---|---|
| $\beta_1$ | $0.2$ day$^{-1}$ | Fitted to data |
| $\beta_2$ | $0.0330$ day$^{-1}$ | Fitted to data |
| $v$ | Variable | Assumed |
| $\theta$ | $1/84$ day$^{-1}$ | Assumed |
| $\eta_1$ | 0.463 | [25] |
| $\eta_2$ | 0.557 | [25] |
| $w$ | $0.25$ day$^{-1}$ | [24] |
| $p_1$ | 0.12 | [21] |
| $p_2$ | 0.089 | Estimated |
| $\delta_1$ | $3.2135 \times 10^{-3}$ day$^{-1}$ | Fitted to data |
| $\delta_2$ | 0 | Assumed |
| $\gamma$ | $3.6987 \times 10^{-2}$ day$^{-1}$ | Fitted to data |

# 4 Numerical simulations

In this section, we perform some numerical simulations for model (1) to provide estimates for the evolution of the COVID-19 outbreak in Mexico.

## 4.1 Data fitting and estimation of parameters

We used cumulative data provided by the Johns Hopkins University repository [23] to fit the parameters of model (1) in the absence of vaccination. We considered the data for reported COVID-19 infections, deaths and recovered cases during the period from 12 November 2020 to 24 December 2020, which is before the vaccination program in Mexico began.

For this part, we considered system (1) with $v = 0$ and the vaccinated subpopulations $V_1$, $V_2$, $E_V$, $A_V$ and $I_V$ equal to zero. We regarded as fixed parameters $w = 0.25$, which corresponds to a latent period of 4 days [24], and a proportion $p_1 = 0.12$ of symptomatic infections [21]. The set of differential equations was solved using Matlab 2016b with the ode45 solver, and the values for $\beta_1$, $\beta_2$, $\delta_1$ and $\gamma$ were estimated by fitting the model solutions to the above mentioned dataset using the method described in [21]. The best fit values for these parameters are shown in Table 1. Figure 2 depicts a comparison between the model solutions and the observed cumulative COVID-19 data before the vaccination period.

## 4.2 Simulations for the model with vaccination

We will now simulate the solutions to model (1) to assess the impact of the vaccination program that started in Mexico in December 2020 to combat the COVID-19 pandemic.

As of early April 2021, five COVID-19 vaccines have received Emergency Use Authorization for their deployment in Mexico: BNT162b2 (Pfizer–BioNTech), AZD1222

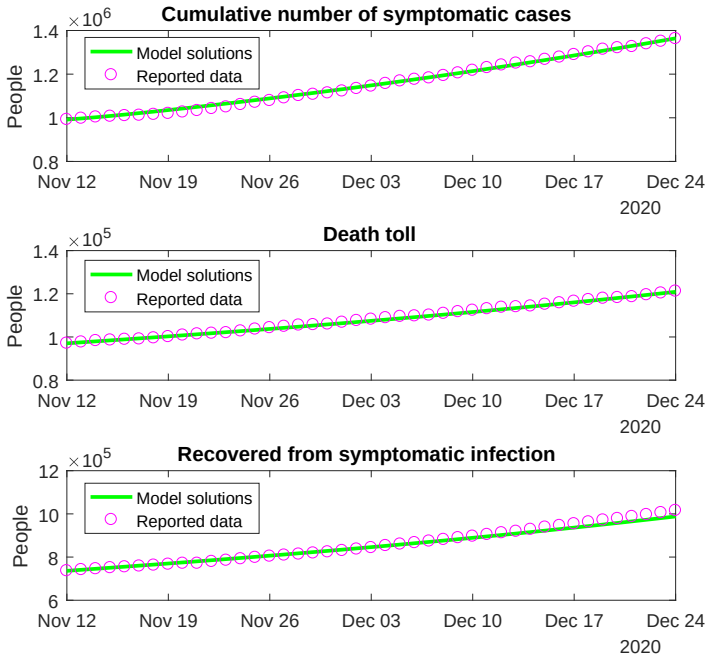


Figure 2: Reported cumulative number of symptomatic cases, COVID-19 deaths and recovered cases in Mexico for the pre-vaccination period, and simulations using model (1) with the parameters in Table 1 and $v = 0$.

Table 2: Estimated values for the vaccination rate $v$.

| Date | Value ($\text{day}^{-1}$) |
|---|---|
| 24 Dec. 2020 – 11 Jan. 2021 | $4.0 \times 10^{-5}$ |
| 12 Jan. 2021 – 15 Jan. 2021 | $7.9 \times 10^{-4}$ |
| 16 Jan. 2021 – 14 Feb. 2021 | $6.0 \times 10^{-5}$ |
| 15 Feb. 2021 – 7 Mar. 2021 | $7.3 \times 10^{-4}$ |
| 8 Mar. 2021 – 14 Mar. 2021 | 0.0021 |
| 15 Mar. 2021 – 31 Mar. 2021 | 0.0017 |

(Oxford–AstraZeneca), Sputnik V (Gamaleya Institute), CoronaVac (Sinovac) and Ad5-nCoV (CanSino); all of them except the last one require two doses [26].

Efficacy estimates for each vaccine based on data from clinical trials are subject to change with the emergence of new analyses. An interim analysis for the Oxford–AstraZeneca vaccine [25] estimated an efficacy against infection (symptomatic or asymptomatic) of 46.3% (31.8%–57.8%), considering people who had a nucleic acid amplification test (NAAT)-positive swab more than 21 days after a single dose, and 55.7% (41.1%–66.7%) for people who tested positive more than 14 days after a second dose of the vaccine. However, a more recent study [27] estimated an efficacy of 63.9% (46.0%–76.9%) after one dose and 59.9% (35.8%–75.0%) after two standard doses given 12 or more weeks apart.

Due to longer dose intervals being associated with greater efficacy against symptomatic infection, the WHO has recommended to administer the Oxford–AstraZeneca vaccine with an interval of 8 to 12 weeks between first and second doses [28]. Based on the above, we will assume in our simulations an average length of $1/\theta = 84$ days for the inter-dose period, and we will use $\eta_1 = 0.463$ and $\eta_2 = 0.557$ as baseline values for the efficacy parameters.

For computing the proportion of infectious vaccinated individuals that show symptoms of the disease ($p_2$), we follow [25], who reported 37 cases of symptomatic COVID-19 disease out of a total of 68 NAAT-positive swabs in the group of people vaccinated with AZD1222, and 112 symptomatic cases out of 153 NAAT-positive cases in the control group. This yields a reduction from 0.732 to 0.544 in the symptomatic proportion after vaccination. Since we have chosen $p_1 = 0.12$, we will take $p_2 = 0.089$ so that $p_1 : p_2 = 0.732 : 0.544$. Furthermore, we assume that the death rate $\delta_2$ of infectious vaccinated people is zero since it is widely accepted that current anti-COVID vaccines provide full protection against severe infections.

We used the daily data on COVID-19 vaccinations in Mexico obtained from [29] to estimate the value of the vaccination rate $v$ over six different date ranges, as shown in Table 2. We plot in Figure 3 a comparison of the reported number of vaccinated people and the simulations obtained with model (1) for the period 24 December 2020 – 31 March 2021. In these graphs, we considered the total population of Mexico as 127 090 000 people.

In order to obtain long-term projections for the vaccination coverage in Mexico, we simulated two different scenarios. First, we assumed that the vaccination rate is kept constant at its baseline value on 31 March 2021 (0.17% of susceptible population per day, which equals roughly 175 000 first doses applied every day for an estimated susceptible

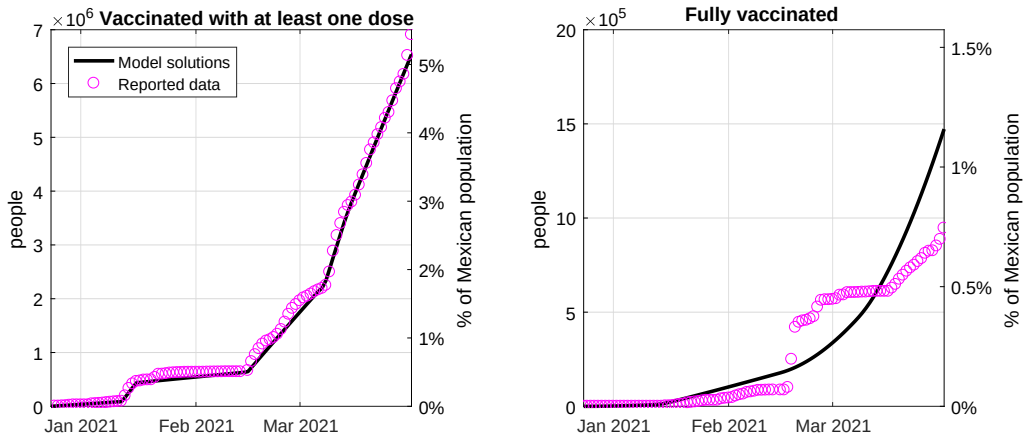


Figure 3: COVID-19 vaccination coverage in Mexico from 24 December 2020 to 31 March 2021. Circles represent real data, continuous lines represent model simulations using the vaccination rate in Table 2.

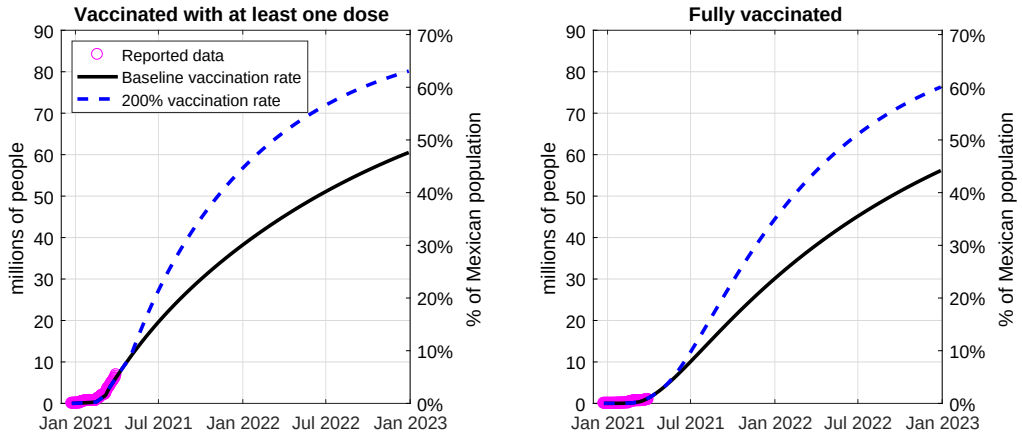


Figure 4: Long-term projections of COVID-19 vaccination coverage in Mexico. Circles represent real data, continuous lines represent simulations using the baseline vaccination rate, and dashed lines represent simulations using 200% vaccination rate from May 2021 onwards.

population of 103 million people). Second, we assumed that the vaccination rate increases to twice its baseline value starting on May 2021 (which translates to slighly more than 300 000 first doses per day). Figure 4 shows that, if vaccines continue to be delivered at their baseline rate, only about 48% of Mexican population will have received their first dose by January 2023, while only 44% will be fully vaccinated by that date. On the other hand, if the vaccination rate is doubled, around 63% of the population will be vaccinated with at least one dose and 60% with two doses by the same date.

### 4.2.1 Assessing the effect of vaccination and different transmission rates

We will next compute the solutions of model (1) to simulate the evolution of the pandemic in Mexico as the vaccination campaign takes place. We consider the initial date for simulations as 24 December 2020. Based on the results obtained in Subsection 4.1, we use the initial conditions

$$S(0) = 1.1622 \times 10^8, \quad E(0) = 3.4415 \times 10^5, \quad I(0) = 2.1247 \times 10^5,$$
$$A(0) = 1.6521 \times 10^6, \quad R(0) = 8.5421 \times 10^6, \quad D(0) = 1.2128 \times 10^5,$$

and $V_1(0) = V_2(0) = E_V(0) = I_V(0) = A_V(0) = 0$. In these subsection, we will consider different values for the transmission rates $\beta_1$ and $\beta_2$ to account for the possibility that the number of infectious contacts between people may increase or decrease due to resumption of economical activities, compliance with social/physical distancing, wearing of face masks, etc. Hence, we consider three cases: when $\beta_1$ and $\beta_2$ are kept with the values in Table 1, when both of them decrease to an 80% of these values, and when they increase to a 120%. The values for other parameters are fixed as in Tables 1 and 2.

Figure 5 depicts the time evolution of the number of infectious COVID-19 cases with symptoms ($I(t) + I_V(t)$) and the death toll ($D(t)$) for each of the above cases. In each graph, we have plotted the solutions assuming the baseline vaccination rate and the 200% vaccination rate, as well as a counterfactual case with no vaccination.

Figure 5(a) shows that, in the case of low transmission rate, the number of active cases would start to decrease in the early months of 2021, and the epidemic would be almost extinguished by March 2022. In the cases with higher transmission rate (Figures 5(b) and (c)), the epidemic curve would reach its peak around May 2021, and the number of active symptomatic cases would be less than 1000 by September 2022. Figures 5(d)–(f) show that the cumulative number of deaths would be around 270 000 for low transmission, more than 400 000 for baseline transmission, and more than 600 000 for high transmission rate.

We can also see that an increase in the vaccination rate to double its baseline value will result in 36 000 less deaths than in the baseline case (Figure 5(e)). However, comparing Figures 5(d) and (e) shows that more than 160 000 deaths can be avoided by reducing the transmission rate to 80%, while a 20% increase in the transmission rate would result in 200 000 additional deaths (Figure 5(f)). This suggest that decreasing the number of infectious contacts by complying with preventive measures is more effective than simply accelerating the deployment of vaccines.

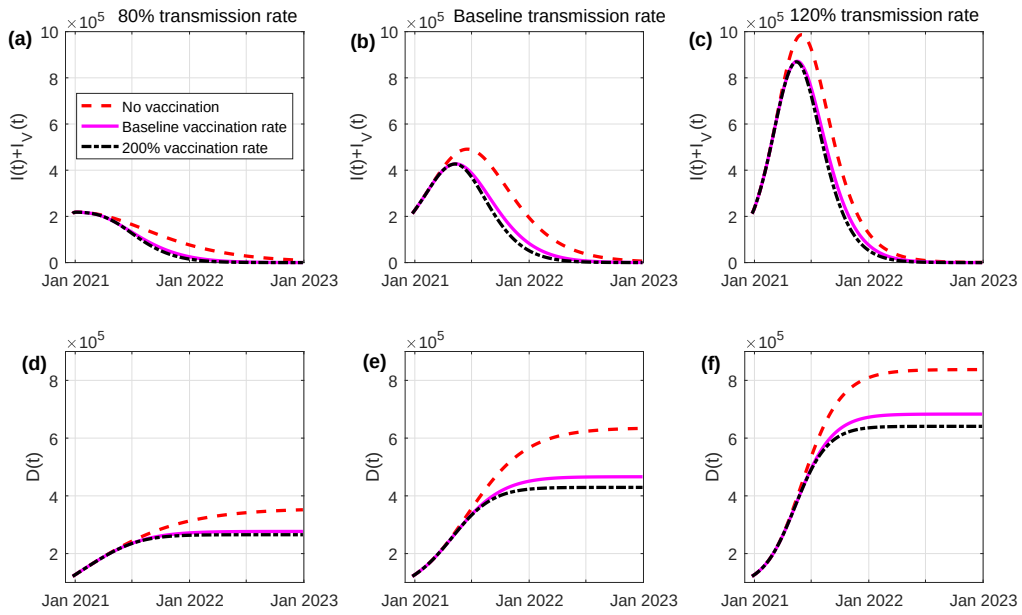


Figure 5: Simulations of model (1) using different values for the transmission rates. (a) and (d): 80% transmission rate. (b) and (e): baseline transmission rate. (c) and (f): 120% transmission rate. Top row: number of active symptomatic infectious cases. Bottom row: Cumulative number of deaths.

### 4.2.2 Assessing the effect of different vaccine efficacy rates

Given that there is still uncertainty regarding the efficacy of anti-COVID vaccines against infection, including asymptomatic cases, we will also simulate the solutions of model (1) using different values for the parameters $\eta_1$ and $\eta_2$.

Figure 6 shows the number of active infectious cases with symptoms $(I(t)+I_V(t))$ and without symptoms $(A(t)+A_V(t))$, as well as the death toll $(D(t))$, using different efficacy rates: in addition to the baseline case ($\eta_1 = 0.463$, $\eta_2 = 0.557$), we include a case with lower efficacy ($\eta_1 = 0.4$, $\eta_2 = 0.45$) and a case with higher efficacy ($\eta_1 = 0.6$, $\eta_2 = 0.65$). For these simulations, we plotted all solutions using baseline vaccination rate. We can see that lower efficacy results in an additional 11 903 symptomatic cases (2.83% increase) and 118 387 asymptomatic cases (3.52% increase) at the peak of the infection curve, compared with the case with higher efficacy. However, this does not significantly affect the time when the peak occurs. Lower efficacy also results in 20 058 additional deaths.

## 4.3 Impact of vaccination coverage on the control reproduction number

Next, we will study how the control reproduction number $\mathcal{R}_c$ is affected by some of the model parameters.

By equation (3), we know that $\mathcal{R}_c$ does not only depend on the parameters of system (1), but also on the final proportions of unvaccinated susceptible people $(S^*/N^*)$ and fully

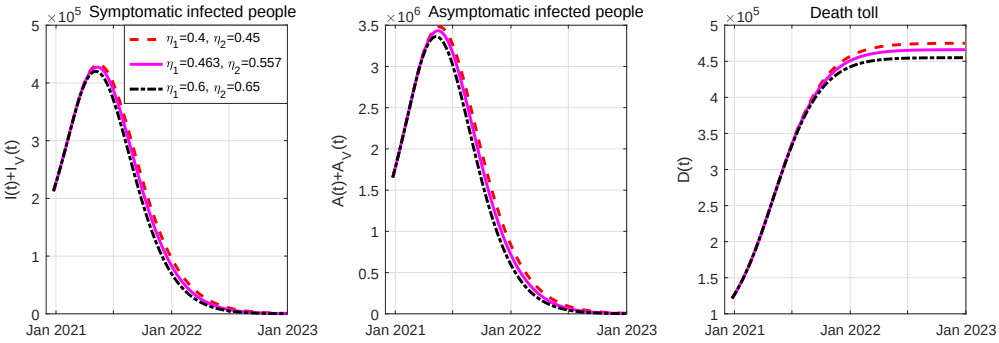


Figure 6: Simulations of model (1) using different values for the vaccine efficacy rates. Left panel: number of active symptomatic infectious cases. Central panel: number of active asymptomatic infectious cases. Right panel: cumulative death toll.

vaccinated people ($V_2^*/N^*$) at the time when vaccines are no longer being deployed to the population.

We recall that a disease-free equilibrium takes the form $P_0 = (S^*, 0, 0, 0, 0, V_2^*, 0, 0, 0, R^*)$, where the total population is $N^* = S^* + V_2^* + R^*$. If we define

$$x = \frac{V_2^*}{N^*} \quad \text{(the proportion of vaccinated people)},$$
$$y = \frac{R^*}{N^*} \quad \text{(the proportion of people recovered from the disease)},$$

we can rewrite the expression for the control reproduction number as

$$\mathcal{R}_c(x,y) = \left[\frac{\beta_1 p_1}{\delta_1+\gamma} + \frac{\beta_2(1-p_1)}{\gamma}\right](1-x-y) + (1-\eta_2)\left[\frac{\beta_1 p_2}{\delta_2+\gamma} + \frac{\beta_2(1-p_2)}{\gamma}\right]x.$$

Figure 7 depicts the value of $\mathcal{R}_c$ as function of the proportions $x$ and $y$, using several values for the transmission rates and efficacy after the second vaccine dose. Other parameter values were taken as in Table 1. We can see that an increase in either $x$ or $y$ contributes to reducing the reproduction number, and therefore, is helpful towards achieving herd immunity.

Herd immunity occurs when a large portion of the population has become immune to the disease due to vaccination or natural recovery, which makes spread of the disease difficult. Thus, the minimal level of vaccination coverage that is required to achieve herd immunity (that is, making $\mathcal{R}_c < 1$) will also depend on the percentage of the population that has been infected and then successfully recovered. Comparing the different panels of Figure 7, we can see that increasing the vaccine efficacy $\eta_2$ reduces the vaccination coverage needed to make $\mathcal{R}_c < 1$ for a fixed proportion of recovered people. However, this reduction is small compared to the effect gained by decreasing the transmission rate. For example, when $\eta_2 = 0.65$ and the recovered population is close to zero, it is necessary to vaccinate 60% of population to obtain $\mathcal{R}_c = 1$ in the case of 120% transmission rate, 40% in the case of baseline transmission rate, and only 14% of population in the case of 80% transmission rate (bottom row of Figure 7).

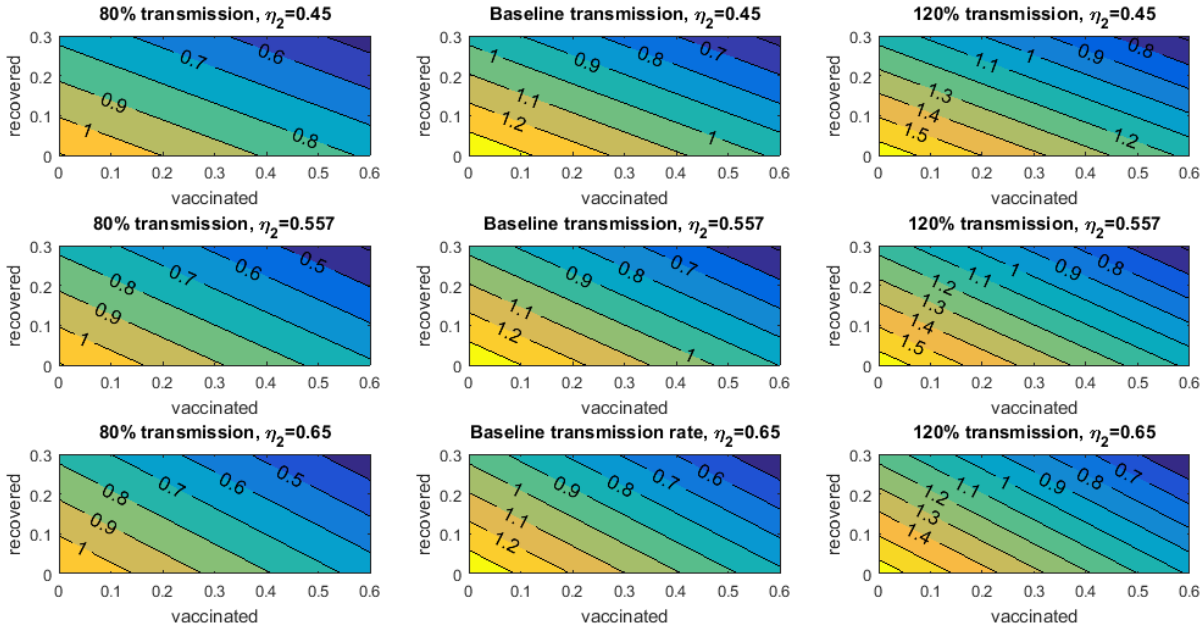


Figure 7: Value of the control reproduction number as function of the proportion of fully vaccinated individuals (horizontal axis) and recovered individuals (vertical axis).

# 5 Conclusion

In this work, we studied a model for COVID-19 with vaccination. Our work was based on the SEIARD model proposed in [21], which included an exposed (latent) compartment and different transmission rates for the symptomatic and asymptomatic infectious individuals; we extended this model by incorporating vaccinated compartments and considering a two-dose vaccination regime.

We showed that our model has multiple disease-free equilibria and computed the control reproduction number $\mathcal{R}_c$ using the next-generation matrix method. We established that the set of disease-free equilibria is locally asymptotically stable when $\mathcal{R}_c < 1$ and unstable when $\mathcal{R}_c > 1$. Furthermore, we determined a condition that guarantees the global asymptotic stability of the DFE.

We performed a numerical simulation on our model using repository data on the outbreak of COVID-19 in Mexico and the daily data on COVID-19 vaccinations to estimate the value of the vaccination rate over six different date ranges. We used the efficacy estimates based on data from clinical trials of the Oxford–AstraZeneca vaccine, which is the one that is being more widely distributed in Mexico at the time of this writing. We remark that, in this article, we considered *vaccine efficacy* in the sense of protection against COVID-19 infection (symptomatic or asymptomatic), while other works consider efficacy as protection against symptomatic infection only.

In order to obtain long-term projections for the vaccination coverage, we simulated two different scenarios. First, we assumed that the vaccination rate is kept constant by vaccinating the same proportion of susceptible population per day, and secondly, we assumed that the vaccination rate increases to twice its baseline value. Our study showed that if vaccines continue to be delivered at their baseline rate, only about 48% (less than

half) of the Mexican population will have received their first dose by January 2023, and only 44% will be fully vaccinated by that date. On the other hand, if the vaccination rate is doubled, around 63% of the population will be vaccinated with one dose and 60% with two doses. In the case of low transmission rate, the number of active cases would start to decrease in the early months of 2021, and the epidemic would be almost eradicated in early 2022, while in the cases with medium to high transmission rate the epidemic curve would reach its peak around May 2021 and would be close to zero by late 2022.

Our simulations show that keeping a low transmission rate (by wearing face masks, complying with social/physical distancing, etc.) is the most effective method to reduce the death toll. For example, reducing the transmission rate to 80% its baseline value results in 160 000 less deaths, while doubling the vaccination rate results in only 36 000 less deaths. Also, decreasing the transmission rate is more effective to reduce the control reproduction number and achieve herd immunity than using vaccines with higher efficacy rates. However, accelerating the application of vaccines, combined with maintaining a low transmission rate by following preventive measures would result in an even better strategy for curtailing the pandemic and reducing the number of deaths.

# References

1. World Health Organization. *WHO advisory committee on variola virus research: report of the thirteenth meeting* tech. rep. (World Health Organization, 2011). <https://apps.who.int/iris/handle/10665/70778>.
2. Cai, L.-M., Li, Z. & Song, X. Global analysis of an epidemic model with vaccination. *Journal of Applied Mathematics and Computing* **57,** 605–628 (2018).
3. Anderson, R. M. & May, R. M. *Infectious Diseases of Humans: Dynamics and Control* (Oxford University Press, 1991).
4. Kribs-Zaleta, C. M. & Martcheva, M. Vaccination strategies and backward bifurcation in an age-since-infection structured model. *Mathematical Biosciences* **177,** 317–332 (2002).
5. Scherer, A. & McLean, A. Mathematical models of vaccination. *British Medical Bulletin* **62,** 187–199 (2002).
6. Arino, J., McCluskey, C. C. & van den Driessche, P. Global results for an epidemic model with vaccination that exhibits backward bifurcation. *SIAM Journal on Applied Mathematics* **64,** 260–276 (2003).
7. Alexander, M. E. *et al.* A vaccination model for transmission dynamics of influenza. *SIAM Journal on Applied Dynamical Systems* **3,** 503–524 (2004).
8. Gumel, A. B., McCluskey, C. C. & Watmough, J. An SVEIR model for assessing potential impact of an imperfect anti-SARS vaccine. *Mathematical Biosciences & Engineering* **3,** 485 (2006).
9. Martcheva, M. in *Current Developments in Mathematical Biology* (eds Mahdavi, K., Culshaw, R. & Boucher, J.) 149–172 (World Scientific, 2007).

10. Buonomo, B. & Della Marca, R. Oscillations and hysteresis in an epidemic model with information-dependent imperfect vaccination. *Mathematics and Computers in Simulation* **162,** 97–114 (2019).

11. Widyaningsih, P., Candrawati, P., Sutanto & Saputro, D. R. S. Maternal antibody Susceptible Vaccinated Infected Recovered (MSVIR) model for tetanus disease and its applications in Indonesia. *Journal of Physics: Conference Series* **1306,** 012002 (2019).

12. Sulayman, F., Abdullah, F. A. & Mohd, M. H. An SVEIRE model of tuberculosis to assess the effect of an imperfect vaccine and other exogenous factors. *Mathematics* **9,** 327 (2021).

13. Moore, S., Hill, E. M., Tildesley, M. J., Dyson, L. & Keeling, M. J. Vaccination and non-pharmaceutical interventions for COVID-19: a mathematical modelling study. *The Lancet Infectious Diseases* (2021).

14. Saad-Roy, C. M. *et al.* Epidemiological and evolutionary considerations of SARS-CoV-2 vaccine dosing regimes. *Science* (2021).

15. Gog, J. R., Hill, E. M., Danon, L. & Thompson, R. Vaccine escape in a heterogeneous population: insights for SARS-CoV-2 from a simple model. *medRxiv.* doi:https://doi.org/10.1101/2021.03.14.21253544 (2021).

16. Tang, B. *et al.* The minimal COVID-19 vaccination coverage and efficacy to compensate for potential increase of transmission contacts, and increased transmission probability of the emerging strains. *Research Square.* doi:https://doi.org/10.21203/rs.3.rs-140717/v1 (2021).

17. Aruffo, E. *et al.* Community structured model for vaccine strategies to control COVID19 spread: a mathematical study. *medRxiv.* doi:https://doi.org/10.1101/2021.01.25.21250505 (2021).

18. Alvarez, M. M., Bravo-González, S. & Trujillo-de Santiago, G. Modeling the effect of vaccination strategies in an Excel spreadsheet: The rate of vaccination, and not only the vaccination coverage, is a determinant for containing COVID-19 in urban areas. *medRxiv.* doi:https://doi.org/10.1101/2021.01.06.21249365 (2021).

19. Salcedo-Varea, G. A., Peñuñuri, F., González-Sánchez, D. & Díaz-Infante, S. Optimal piecewise constant vaccination and lockdown policies for COVID-19. *medRxiv.* doi:https://doi.org/10.1101/2021.01.13.21249773 (2021).

20. Avila-Ponce de León, U., Pérez, Á. G. C. & Avila-Vales, E. An SEIARD epidemic model for COVID-19 in Mexico: mathematical analysis and state-level forecast. *Chaos, Solitons & Fractals* **140,** 110165 (2020).

21. Avila-Ponce de León, U., Pérez, Á. G. C. & Avila-Vales, E. A data driven analysis and forecast of an SEIARD epidemic model for COVID-19 in Mexico. *Big Data and Information Analytics* **5,** 14–28 (2020).

22. Van den Driessche, P. & Watmough, J. Reproduction numbers and sub-threshold endemic equilibria for compartmental models of disease transmission. *Mathematical Biosciences* **180,** 29–48 (2002).

23. Johns Hopkins CSSE. *2019 Novel Coronavirus COVID-19 (2019-nCoV) Data Repository.* Accessed on 26 February 2021. <https://github.com/CSSEGISandData/COVID-19>.

24. Sjödin, H., Wilder-Smith, A., Osman, S., Farooq, Z. & Rocklöv, J. Only strict quarantine measures can curb the coronavirus disease (COVID-19) in Italy, 2020. *Eurosurveillance* **25,** 2000280 (2020).

25. Voysey, M. *et al.* Safety and efficacy of the ChAdOx1 nCoV-19 vaccine (AZD1222) against SARS-CoV-2: an interim analysis of four randomised controlled trials in Brazil, South Africa, and the UK. *The Lancet* **397,** 99–111 (2021).

26. Government of Mexico. *Vacunación COVID.* Accessed on 6 April 2021. <https://coronavirus.gob.mx/vacunacion-covid>.

27. Voysey, M. *et al.* Single-dose administration and the influence of the timing of the booster dose on immunogenicity and efficacy of ChAdOx1 nCoV-19 (AZD1222) vaccine: a pooled analysis of four randomised trials. *The Lancet* **397,** 881–891 (2021).

28. World Health Organization. *The Oxford/AstraZeneca COVID-19 vaccine: what you need to know.* Accessed on 25 March 2021. <https://www.who.int/en/news-room/feature-stories/detail/the-oxford-astrazeneca-covid-19-vaccine-what-you-need-to-know>.

29. Roser, M., Ritchie, H., Ortiz-Ospina, E. & Hasell, J. Coronavirus Pandemic (COVID-19). *Our World in Data.* <https://ourworldindata.org/coronavirus> (2020).